Effect of Anode Composition on Tungsten Arc Characteristics

Relatively minor changes in anode composition cause significant changes in the arc potential-arc current characteristics of inert gas shielded tungsten arcs.

BY THEODORE F. CHASE, JR. AND WARREN F. SAVAGE

ABSTRACT. The effect of alloy composition on the propensity for hot cracking has received considerable study. However, little effort has been expended in investigating the influence of alloy composition on the fusion zone dimensions and weld penetration. The welding arc has been investigated and analyzed by many investigators. Unfortunately many of the reports studying the arc have depended upon or have reported facts concerning arc phenomena which may not apply to the actual welding process. It is interesting to note that few reports have been published which consider the behavior of an actual welding arc. For example, quantitative descriptions of the arc arrived at by calorimetric means, studies of high-current short duration arcs and low-current long-arc-gap carbon arcs may not be applicable to welding arcs. These variations in experimental techniques have also produced disagreement among investigators regarding the role the anode plays in a welding arc.

This investigation consists of a study of the effect of anode composition on the arc

T. F. CHASE and W. F. SAVAGE are with Rensselaer Polytechnic Institute, Troy, New York.

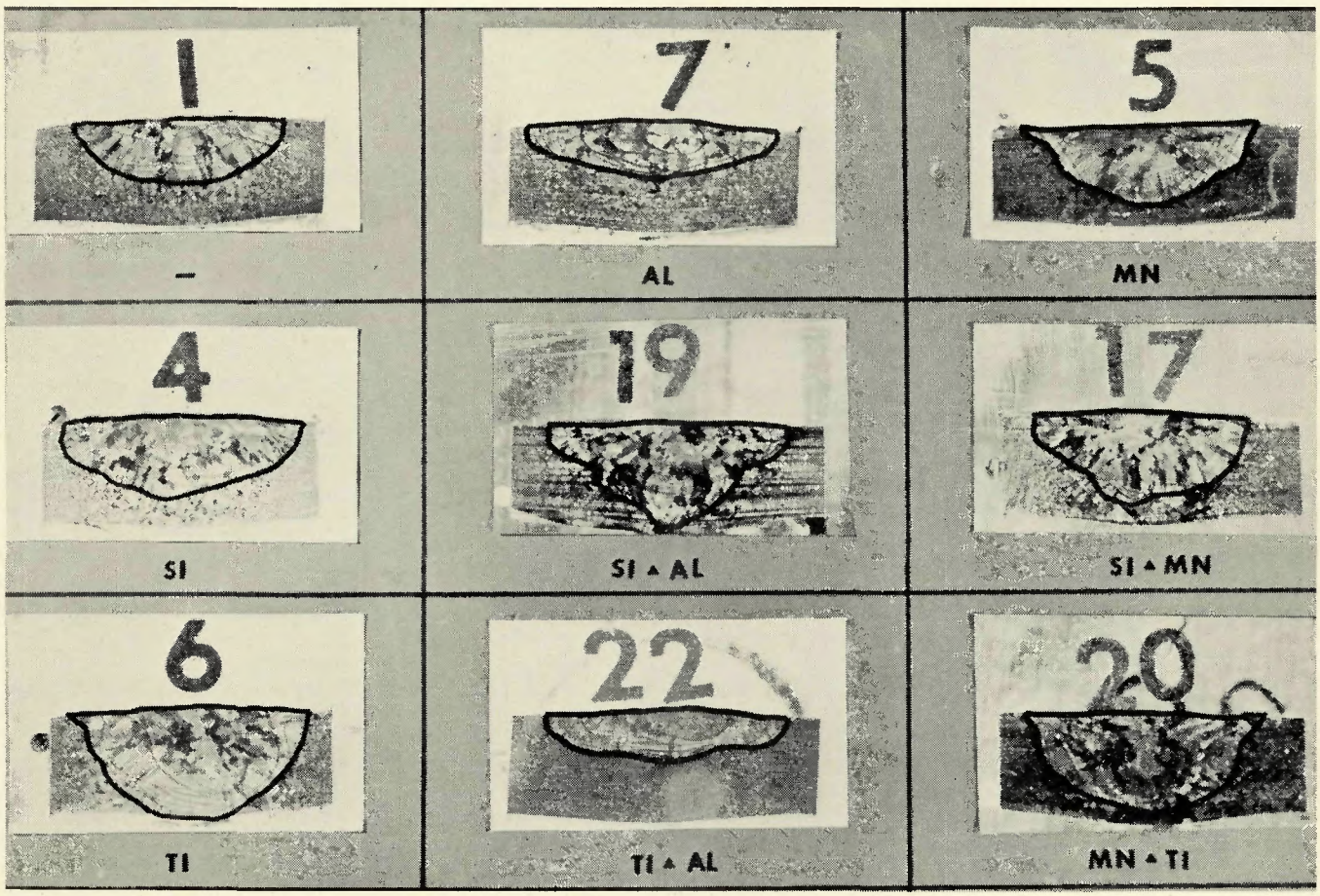

Fig. 1—Cross-sections of fusion welds in Inconel 600 with selected element additions

Table 1—Composition of Fusion Zone in Weld Specimens Shown In Fig. 1

Alloying element	Identification number 1	4	5	6	7	17	19	20	22
Fe %	9.63	9.47	10.1	10.6	9.52	9.79	9.92	10.3	9.23
Cr	14.8	14.8	14.6	14.9	14.8	14.6	14.8	14.8	14.5
Ni	74.5	73.8	74.1	73.6	73.6	75.3	74.5	74.3	75.0
S	0.005	0.004	0.013	0.004	0.004	0.004	0.004	0.005	0.004
P	0.001	0.001	0.001	0.002	0.002	0.0007	0.0005	0.0009	0.001
Si	0.007	0.14	0.07	0.08	0.06	0.29	0.23	0.07	0.07
Mn	0.056	0.042	0.900	0.074	0.045	1.50	0.050	1.30	0.060
Ti	0.02	0.02	0.02	0.22	0.02	0.01	0.01	0.30	0.35
Al	0.03	0.03	0.03	0.03	0.30	0.03	0.21	0.03	0.33
C	0.003	0.004	0.002	0.002	0.002	0.002	N.A.	N.A.	0.003
Cu	0.016	0.012	0.012	0.014	0.013	0.01	0.01	0.01	0.014

Table 2—Summary of Dimensions of Welds and Element Additions Involved

Identification	Depth of penetration cm	Cross-sectional area sq cm	Element added
1	0.379	0.445	None
4	0.475	0.616	Si (0.14%)
5	0.467	0.552	Mn (0.9 %)
6	0.635	0.758	Ti (0.22%)
7	0.344	0.458	Al (0.30%)
17	0.537	0.575	Si (0.29%) Mn (1.50%)
19	0.635	0.633	Si (0.23%) Al (0.21%)
20	0.546	0.685	Mn (1.30%) Ti (0.30%)
22	0.291	0.302	Ti (0.35%) Al (0.33%)

potential-arc current characteristic curve. Precautions were taken to assure that equivalent experimental procedures were followed for all runs and typical welding parameters were used. To minimize the complex interaction effects one would have in investigating a multicomponent alloy such as stainless steel, single element additions were made to high purity nickel. These minor element additions were found to influence an argon-shielded tungsten arc considerably.

The arc potential at a given current and arc length was altered by changing the anode composition. The slope of the arc potential-arc current characteristic curve was also found to be influenced by the element addition. Although no simple correlation was found between the observed arc characteristics and the physical properties of the minor alloying additions, the observed effects are believed to be of significant practical importance. A second paper, currently in preparation will describe the results of a study of the voltage distribution in a GTA arc which was performed as part of the investigation of the effect of anode composition on tungsten arc characteristics.

Introduction

Weldability as defined by AWS is "the capacity of a metal or combination of metals to be welded under fabrication conditions into a specific suitably designed structure and to perform satisfactorily in the intended service." Weldability of materials has been the subject of innumerable investigations since Nikolas Von Bernardos and Stanislov Olczewski received their patent in the field of arc welding in 1885. During the past decade great strides have been made in relating weldability to the chemical composition of the weldment and base material.

Hot cracking propensity is one criterion often chosen as a means of evaluating weldability. It is generally agreed that hot cracking occurs above the solidus temperature of the lowest melting phase present.[2] The effect of alloy composition on the propensity for hot cracking has received considerable study.[3, 4, 5] However, the influence of alloy composition on the fusion zone dimensions and weld penetration should also be included in any list of considerations for judging a material's weldability. Unfortunately, little effort has been expended in investigating the effects of material composition on fusion zone dimensions.

Observations have been reported by Oyler[6] et al, Goodwin[4], and Ludwig[7] concerning differences in fusion zone dimensions as a result of minor composition variations. These investigations involved complex alloys but the consensus of the authors was that minor compositional variations markedly influenced the melting efficiency of the gas tungsten arc (GTA) process.

Since the present investigation also involves the GTA process, a brief review of earlier welding arc investigations is warranted.

Welding Arc Physics

One of the first reviews on the welding arc was by Spraragen and Lengyel[8] and a more recent one was prepared by Jackson.[1] Jackson states, "A welding arc consists of a sustained electrical discharge through a high temperature conducting plasma, producing sufficient thermal energy so as to be useful for the joining of metal by fusion."

The welding arc has been analyzed by many investigators. Unfortunately many of the reports studying the welding arc have depended upon or have reported facts concerning arc phenomena which may not apply to the actual welding process. It is interesting to note that few reports have been published which consider the behavior of an actual welding arc. For example, quantitative descriptions of the arc arrived at by calorimetric means[9, 10, 11, 12] studies of high-current short duration arcs[13] and low-current long-arc-gap carbon arcs[14] may not be applicable to welding arcs.

Goldman and White[15] concluded in their investigation of six anode materials (aluminum, silver, cobalt, copper, tungsten and zinc) that there was no appreciable effect of anode composition on the arc potential-arc current characteristic curve. However, these investigators used anodes so efficiently cooled as to remain solid. Skolnik and Jones[16] have reported that "in the inert gas arc the anode drop is zero or negligibly small." However, they conducted their investigation at arc currents less than 100 amp. In addition Morris and Gore[17] have stated that "the anode plays no part in the arc mechanism except to serve as the positive electrode and there is no reason why the arc mechanism should vary with a change in the anode material." Morris and Gore also reported that "the melting rate of the workpiece is, for a given current, dependent only upon the thickness of the metal and its thermal conductivity, while the arc delivers the same power to the work regardless of the work metal."

Another investigator, Rabkin,[18] states that the anode voltage drop does not depend on the material of which the electrodes are made or on the composition of the gases in the arc column, and is a constant quantity equal to 2.5 $\pm$ 0.2 volts. However, recent investigations by Goodwin[4] and Ludwig[7] conclude that the welding arc is sensitive to the anode material. Ludwig suggested that an energy balance exists at the anode and he postulates the mechanisms by which heat is both supplied to the anode and transferred from the anode to its surroundings. Ludwig suggests that the variations in fusion zone dimensions which he observed for different heats of the same alloy are due to changes in the anode spot size and that this change is related to the amount of easily ionized components present as impurities. Subsequently, Savage et al[19] have postulated that the formation of oxides on the surface of a weld puddle may alter the magnitude of the anode drop. This in

turn could modify the fusion zone dimensions.

Goodwin[4] and Dickinson[20] observed considerable variations in fusion zone dimensions which appeared to be attributable to the concentration of minor elements in Inconel 600. These investigators studied 64 different alloy compositions within the composition limits for Inconel 600. Additions of six minor elements were investigated using a full factorial experimental design. Photomacrographs of the cross sections of typical welds made under identical conditions in 9 of the 64 alloys constituting Goodwin's six factorial experiments are shown in Fig. 1. Table 1 summarizes the chemical compositions of the nine specimens which are identified by the numbers directly above the weld fusion zones in Fig. 1. The underlined compositions represent the intentional additions to the basic ternary, whose composition corresponds to that of Specimen 1.

Table 2 summarizes the depth of penetration and cross-sectional areas of the weld fusion zones shown in Fig. 1. Note that the depth of penetration varies by a factor of $\frac{0.635}{0.294} = 2.18$ (compare Specimens 19 and 22) while the cross-sectional area varies by a factor of $\frac{0.758}{0.302} = 2.51$ (compare Specimens 6 and 22). Of the listed additions, only aluminum and a combination of titanium and aluminum decreased the penetration, while only the combination of titanium and aluminum decreased the cross-sectional area. All other additions summarized in Table 11 increased both the penetration and the cross-sectional area of the fusion zones above the corresponding values for the basic ternary (Specimen 1).

As a result of these and other complex interaction effects noted by Goodwin and the obvious disagreement among investigators regarding the role the anode plays in the arc voltage distribution, it was decided to initiate a comprehensive study of the effect of anode composition on the characteristics of a gas shielded tungsten welding arc.

High purity nickel was chosen as the basic component of the anode in the interest of simplicity and the effect of additions of controlled amounts of selected alloying elements on the arc characteristics was studied. The following report summarizes the objectives of the investigation, the materials and procedures used and the results obtained. The effort was actually divided into two phases: The effect of anode composition on the arc potential-arc current characteristics, while a second paper now in preparation will be concerned with the influence of anode composition on the potential distribution in the arc.

Objective

The objective of this part of the investigation was to study the effect of anode composition on the arc potential-arc current characteristics associated with an inert gas shielded tungsten arc welding process.

Material and Apparatus

High purity nickel bar stock (½ by 2 in.) was selected as the base metal for this investigation to avoid the complex interactions one might encounter with a multi-component material. The chemical analysis of this bar stock is summarized in Table 3. The as-received material had been annealed for 3 hr at 1350F subsequent to cold-rolling to gage.

The composition of the fusion zone of autogenous GTA spot welds was modified by introducing inserts of selected elements in a 1/16 in. diameter by 1/16 in. deep hole drilled in 2 by 2 by ½ in specimens of the high purity bar stock. A plug cut from 1/16 in. nickel wire (composition summarized in Table 3) was then pressed in place to seal the additions from the ambient atmosphere. By positioning the GTA torch directly above the insert, the encapsulated alloy addition was melted and mixed with the high purity base material during the arc on-time, thus creating a molten anode of modified composition.

The elements added to the base material in this fashion were selected according to their availability in pure form and their physical and chemical properties. All elements chosen for addition were of 99.9 % purity or better. Wherever possible, materials available in bulk form were employed as additions to minimize the effect of surface contaminants characteristic of powders (which have an inherently high surface-to-volume ratio).

Table 4 lists the elements chosen as additions and the form in which they were added, together with those physical properties[21, 22] considered to be pertinent. The work functions listed in Table 4 were obtained from Fomenko's handbook which was judged the most recent and authoritative reference. Of the several methods for determining the work function of an element, determinations based upon thermionic measurements were judged most pertinent to this investigation and values obtained by this method are thus cited wherever available. It is of interest to note, however, that significant differences in the reported values of the work functions of some elements were encountered in searching the literature.

Sample Preparation

Figure 2 shows in schematic form the details of the specimens used in this portion of the investigation. Eleven specimens were prepared, each containing a 50 milligram insert of one of the eleven additions listed in Table 4 (including one specimen with only Ni wire added as a control specimen). Whether in bulk or powder form, the insert was compacted in the predrilled hole using a unit pressure of the order of 100,000 psi. A Ni-wire plug was then inserted and peened flush with the surface to seal the compacted insert in place.

Table 3—Chemical Compositions

Base metal	
C	0.03 %
S	0.005
Mn	0.25
Fe	0.04
Cu	0.01
Ni	balance
Nickel-wire plugs	
C	0.03 %
S	0.005
Mn	0.24
Fe	0.07
Cu	0.01
Si	0.36
Ti	3.06
Ni	balance

Table 4—Physical Properties of Anode Components

Element	Form	at. wt.	ϕ (ev)	I.P. (volts)	B.P. (°C)
Al	Bulk	26.97	4.25	5.96	2467
Ca	Powder	40.08	2.80	6.09	1487
Y	Bulk	88.92	3.30	6.58	2927
Cr	Powder	52.01	4.58	6.74	2482
Sn	Bulk	118.70	4.38	7.30	2270
Mn	Powder	54.93	3.83	7.41	2097
Ni-wire	Bulk	58.69	4.58	7.61	2732
Cu	Bulk	63.54	4.40	7.68	2595
Fe	Powder	55.85	4.31	7.83	3000
Si	Powder	28.06	4.80	8.12	2355
Sb	Bulk	121.76	4.08	8.50	1380
	Characteristics of Shielding Gas				
Argon	(99.999%)	39.94		15.68	—185.7

Apparatus

A gas-tight chamber (8 in. long by 6 in. wide by 4 in. high) was constructed of lucite with two 8 by 4 in. plateglass windows serving as the front and rear walls of the chamber in order that high speed motion pictures could be obtained of the arc. A water-filled U-tube manometer was employed to measure chamber pressure during each run. In addition, a dewpoint monitor installed within the chamber was employed to insure that the shielding gas was sufficiently free of moisture to prevent gross oxidation of the molten pool. An exhaust valve connected to the chamber was adjusted to maintain the chamber pressure at a constant level.

Electrical Equipment. All welds were made with straight polarity dc using a 600 amp saturable reactor type power supply in a constant current mode. Electrodes were centerless ground 0.125-in. diameter, 2%-thoriated-tungsten, dressed to a conical tip with a 90 deg apex angle. Direct-inking recorders were used to monitor and record the arc potential and arc current. The current and voltage measurements were made with an accuracy of $\pm \frac{1}{4}\%$ by calibrating the recorders against a suitable laboratory standard.

Experimental Procedure

Pre-Run Procedure

Each specimen received equivalent pre-run preparation, including deburring, degreasing and fixturing. Precautions were taken to assure that equivalent experimental procedures were followed for all runs. These precautions included the establishment of equivalent chamber pressure, arc gap spacing, dew point, cinematographic conditions, recorder calibration, duration of chamber purge and equipment warm-up time.

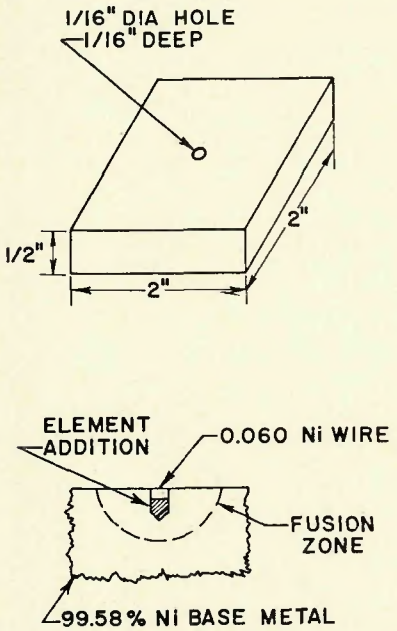

Fig. 2—Schematic representation of sample preparation

Welding Procedure

The welding conditions used for this investigation are listed in Table 5. Prior to making the arc potential-arc current data runs a mixing run was made on each specimen to insure that melting and mixing of the insert material was complete. High-speed movies were taken during this run. Arc potential-arc current characteristic data were obtained by recording the arc voltage as a function of arc current at 25 amp intervals. These data were fed into a computer to generate least-squares analysis plots of arc voltage vs arc current over a range of arc currents extending from 200–350 amp for each specimen.

Results and Discussion

Effect of Additions on Arc Characteristics

Figures 3 to 13 present the arc-potential, arc-current characteristics obtained for the eleven different anode compositions studied. In all cases, the solid circles represent the actual data and the height of the vertical bar through each point corresponds to the 95% confidence limits for the computer generated least squares fit (heavy solid line). In every instance the data fall within the 95% confidence limits for a straight line described by the equation:

$$E = E_{200} - R_p(I - 200) \qquad (1)$$

where: E = arc potential at a current level I (volts); I = arc current (amp); E_{200} = arc potential at 200 amp; R_p = dynamic resistance of the arc.

Figure 3 shows the arc potential as a function of the arc current for the pure nickel anode containing a nickel wire insert used as a control specimen. This arc characteristic is reproduced in Figs. 4 to 13 as a dashed line to permit comparison of each of the other nine arc characteristics with that of the control sample. Inspection of these figures reveals that the 50 mg additions each had a distinctive influence on the arc characteristic. For example, note the curve for an aluminum addition shown in Fig. 4. Although the slope is nearly the same, the arc potential is shifted upward by nearly 0.5 volt over the entire range from 200 to 350 amp. On the other hand, the 50 mg addition of calcium caused a marked change in the slope of the arc characteristic as may be seen by inspecting Fig. 5.

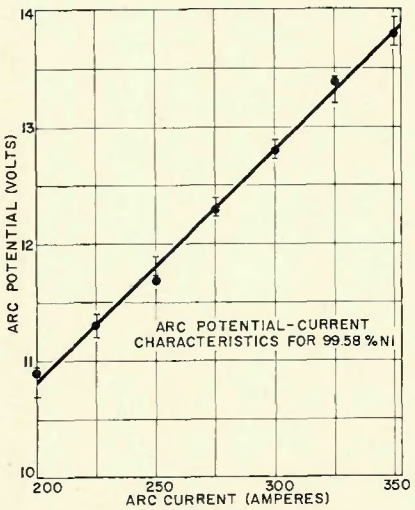

Fig. 3—Arc potential-arc current characteristic curve for 99.58% Ni

The slope of the arc potential, arc current characteristic corresponds to R_p, the dynamic resistance term in Equation 1. The dynamic resistance is defined as the change in arc potential per unit change in arc current and is calculated as follows from the data in Figs. 3 to 13:

$$R_p = \frac{\Delta E}{\Delta I} = \frac{E_{350} - E_{200}}{350 - 200} \qquad (2)$$

where: ΔE = change in arc potential for a given change, ΔI, in arc current; E_{350} = arc potential at 350 amp; E_{200} = arc potential at 200 amp; R_p = dynamic resistance in ohms.

The reciprocal of the dynamic resistance, $\Delta I/\Delta E = 1/R_p$, to borrow a term from vacuum tube technology, may appropriately be termed the "transconductance" of the arc, μ, and would have units of reciprocal ohms, or mhos, if calculated as follows from the data in Figs. 3 to 13:

$$\mu = \frac{\Delta I}{\Delta E} = \frac{350 - 200}{E_{350} - E_{200}} \qquad (3)$$

Table 6 summarizes the values of E_{350}, E_{200}, R_p, and μ obtained from Figs.

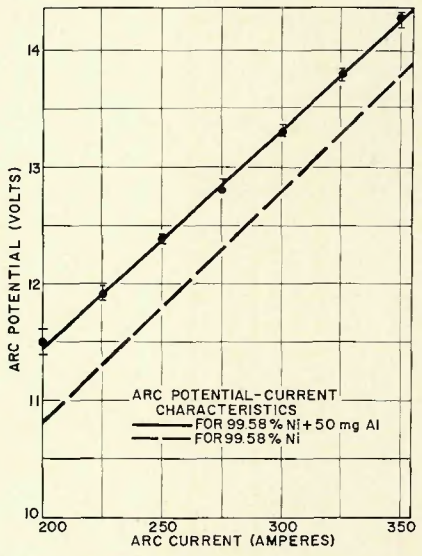

Fig. 4—Arc potential-arc current characteristic curve for 99.58% Ni + 50 mg Al

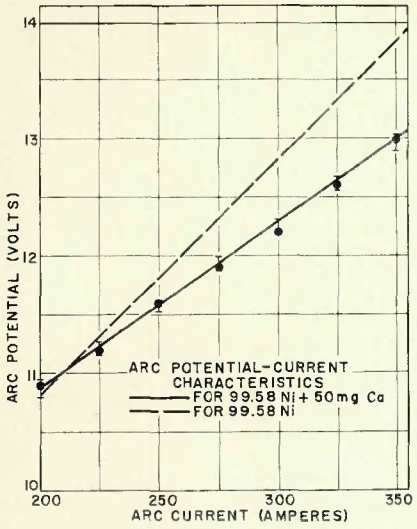

Fig. 5—Arc potential-arc current characteristic curve for 99.58% Ni + 50 mg Ca

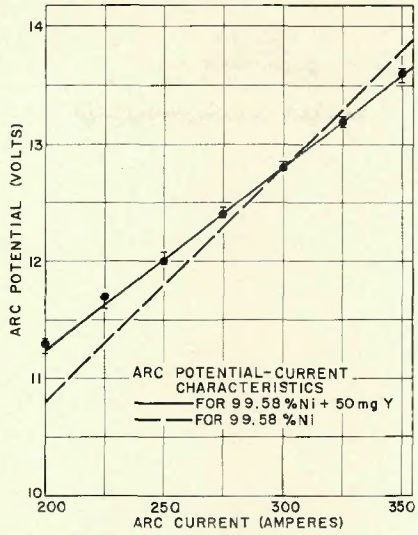

Fig. 6—Arc potential-arc current characteristic curve for 99.58% Ni + 50 mg Y

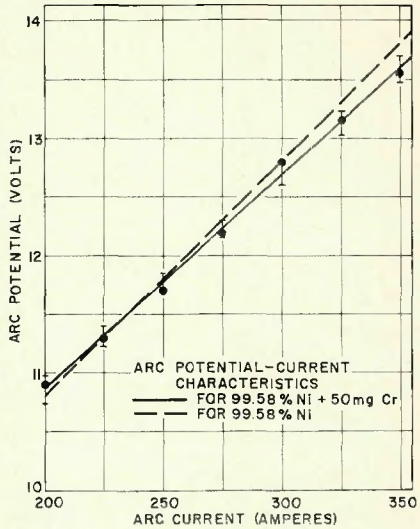

Fig. 7—Arc potential-arc current characteristic curve for 99.58% Ni + 50 mg Cr

3 to 13. The values listed should be compared with the corresponding value for the Ni-wire control specimen to deduce the effect of the individual additives. Note that in no case is the value of E_{200} with an added element less than that for the control specimen. Silicon exerts the greatest influence (+ 1.09 volts), followed in descending order by antimony, copper, manganese and aluminum (both + 0.65 volts), tin, yttrium, iron (+ 0.32 volts). The last two elements, calcium and chromium, have no significant influence on E_{200}.

At a current of 350 amp, silicon, aluminum, antimony, iron, copper, and tin additions increased the value of E_{350}, while calcium, yttrium, chromium and manganese decreased E_{350} below that of the control sample.

The dynamic resistance values, tabulated in milliohms (10^{-3} ohms) for all ten elemental additions are less than the value of 20.0 milliohms observed for the control sample, with calcium having the greatest effect (R_p = 13.9 milliohms) and iron the least (R_p = 19.4 milliohms). The percentage change in R_p (right-hand column in Table 6) ranges from − 30.5% for calcium to − 3.0% for Fe. The values of the transconductance, μ, in mhos show the opposite trend, being the reciprocals of the R_p values. Note that μ varies from a low of 50 mhos for the control sample to a high of 71.94 mhos for calcium.

Table 5—GTA Welding Conditions Used to Obtain Arc Potential-Arc Current Characteristic Curves

Welding current	200 to 350 (25 amp increments)
Welding voltage	(dependent variable)
Arc gap (measured with cold electrode)	0.156 ± 0.002 in.
Stick-out (collet to tip distance)	0.438 ± 0.010 in.
Welding speed	0 (GTA spot weld)
Shielding gas flow	30 cfh argon (99.999% purity)
Chamber pressure:	
prior to run	30 mm H_2O
during run	35 mm H_2O
Chamber dew-point	−64F to −60F
Electrode	1/8 in. diam, 2% thoriated tungsten, ground to conical tip with 90 deg apex angle

Practical Significance

The practical significance of these observations can best be demonstrated by the following hypothetical examples. First, suppose that a GTA process were selected to weld commercially pure nickel using a power supply operating in the constant current mode together with a welding head designed to maintain a constant arc voltage by automatically adjusting the arc length. Assume that a welding current of 300 amp and a welding voltage of 12.8 v was found to provide the desired weld geometry in the pure nickel material used in obtaining the data shown in Fig. 3.

Now suppose that a heat of nickel is obtained with an aluminum content corresponding to that of the specimen used in obtaining the data shown in Fig. 4. Note that for an arc length of 5/32 in., Fig. 4 indicates that this material would exhibit an arc voltage of 13.3 v at 300 amp. Thus the automatic head would decrease the arc length until the preset voltage of 12.8 v was established with the 300 amp welding current. Obviously such a reduction in arc length would decrease the width of the weld pool and increase the depth of penetration. Therefore, the weld in the heat containing aluminum would be narrower and deeper than that in the pure nickel used in establishing the procedure, in spite of the fact that the procedure was followed rigorously.

On the other hand, suppose that the procedure was established for a constant arc length of 5/32 in. with an arc current of 300 amp. Under these condi-

Table 6—Summary of Arc Potential-Arc Current Characteristics

Element added to nickel anode	Arc voltage at 200A E_{200} (volts)	Arc voltage at 350A E_{350} (volts)	Dynamic resistance* R_p (10^{-3} ohms)	Trans-conductance* μ (mhos)	Percentage change in R_p (%)
Al	11.46	14.26	18.7	53.48	− 6.5
Ca	10.87	12.95	13.9	71.94	−30.5
Y	11.27	13.57	15.3	65.36	−23.5
Cr	10.86	13.59	18.2	54.95	− 9.0
Sn	11.405	13.97	17.1	58.48	−14.5
Mn	11.46	13.66	14.7	68.03	−27.0
Ni-wire	10.81	13.81	20.0	50.	Control
Cu	11.53	13.99	16.4	60.98	−18.0
Fe	11.13	14.04	19.4	51.46	− 3.0
Si	11.90	14.39	16.0	62.5	−20.0
Sb	11.58	14.19	17.4	57.47	−13.0

* See text for definition.

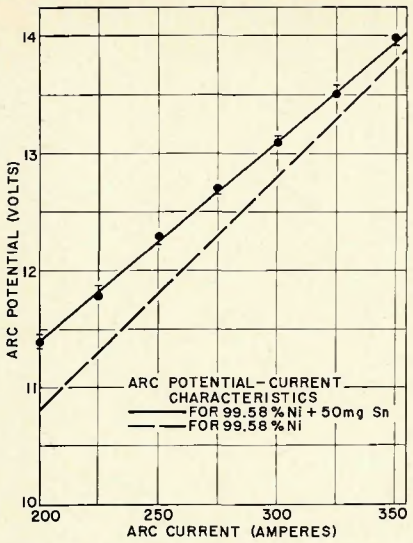

Fig. 8—Arc potential-arc current characteristic curve for 99.58% Ni + 50 mg Sn

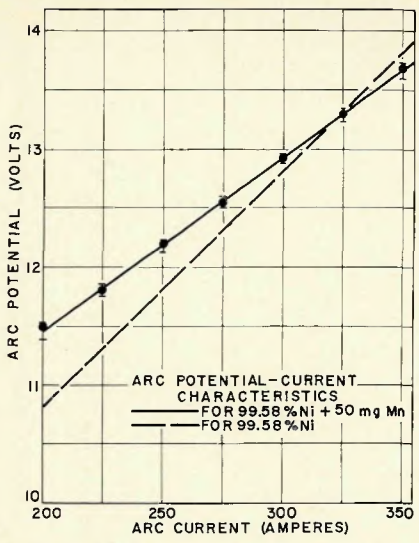

Fig. 9—Arc potential-arc current characteristic curve for 99.58% Ni + 50 mg Mn

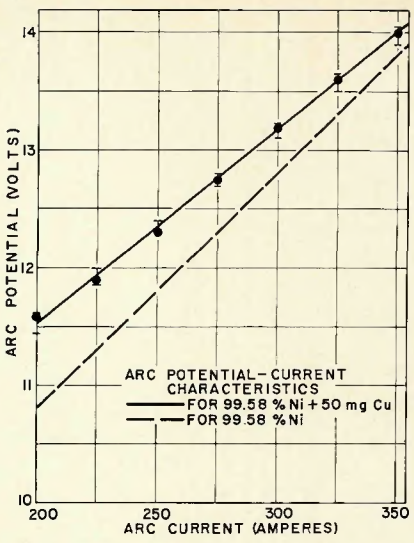

Fig. 10—Arc potential-arc current characteristic curve for 99.58% Ni + 50 mg Cu

tions, the welding voltage of 13.3 v would be 0.5 v higher for the heat containing aluminum than the 12.8 v characteristic of the pure nickel heat used in establishing the procedure. While this is a difference of only 4% in the total arc voltage, the influence of this change on the weld geometry would depend on the region of the arc in which the most significant proportion of the change occurred. For example, if the 0.5 v change was confined to the anode drop region and increased the anode drop from say 3.5 v to 4.0 v, the variation would correspond to a 12.5% change in anode drop, and thus in all probability would cause a significant increase in melting efficiency.

From the above discussion, it is evident that a knowledge of the effect of anode composition on the voltage-current characteristic alone is not sufficient to predict the influence of anode composition on the weld geometry. Rather, one must also determine the effect of the anode composition on the voltage distribution as well. Thus, a more complete analysis of the overall influence of anode composition must be deferred pending publication of the report on the effect of alloying additions on the voltage distribution in an arc. None-the-less, the significance of the data shown in Figs. 2 to 4 should be obvious to the practicing welding engineer.

Possible Influence of Additives

The physical properties of the alloying additions summarized in Table 2 were selected on the basis of their possible influence on the characteristics of a GTA welding arc. Unfortunately, the observed variations in arc characteristics do not seem to bear a straightforward relationship to any of the properties listed. Thus, it is only possible to review the probable role of each of the properties listed and indicate what additional data not currently available may be necessary to explain the observed changes in arc characteristics.

The ionization potential, I.P., of an element in an arc should influence the arc characteristic since metals in general have a much lower ionization potential than the shielding gases used in welding. Morris and Gore[17] have shown that the characteristic curves associated with five different shielding gases possess different slopes and that the curves are shifted to higher voltages according to the ionization potential of the shielding gas. Mantel[23] suggests that metal vapor originating from either of the electrodes increases the conductivity of the arc, because of the lower ionization potentials of the metal vapors. However, the concentration of the added elements is only of the order of 1% in the weld pool and it seems unlikely that this could cause a large enough change in the ionization potential of the plasma. Furthermore, inspection of Table 6 reveals that the variations cannot be correlated with the ionization potential of the additive.

According to the Langevin equation, the mobility of a charged particle is inversely proportional to the mass of the particle. Thus the atomic weight of the metal whose vapor enters the arc should also influence the conductivity of the plasma as a result of the influence of mass on the mobility of the metal ions. However, no correlation with atomic weight appears in the data in Table 6.

The electronic work function, ϕ, of the element addition might also be expected to influence the volt-ampere characteristic of an arc. Specifically, an alloy addition which lowers the work function of the anode should increase the number of secondary electrons contributed to the negatively charged sheath adjacent to the node. Finally, the boiling points of the elemental additions should be considered, since the ease with which an element can leave the anode and enter the plasma as metal vapor should influence the arc characteristic. However, the boiling point of the element itself is not an adequate criterion on which to base the escaping tendency of an atom from a molten binary alloy. This follows since the boiling point of binary systems depends upon the bonding preferences of the elements involved. In general, a preference toward dissimilar bonds would tend to increase the boiling point, whereas a preference for like bonds would tend to decrease the boiling point. Unfortunately, inadequate data on bonding energies prevents quantitative treatment of this problem at this time.

Another circumstance which could influence the escape of the element from the anode to the plasma is the involvement of the element in a chemical reaction at the surface of the weld puddle. A strong tendency for some elements to react with contaminants in the welding atmosphere could fix the element in the form of a stable reaction product on the surface of the molten weld pool. To complicate matters further, stable reaction products floating on the surface of the molten pool have been observed to influence GTA arcs considerably. Similar effects were reported by Wilkinson and Milner[24] and by Savage, et al.[19] Such effects may well influence the heat transfer from the arc to the work in some complex fashion.

There is also the possibility that the surface tension of the molten metal may be changed by the presence of the added element. The nature of this effect would in turn depend upon whether the ele-

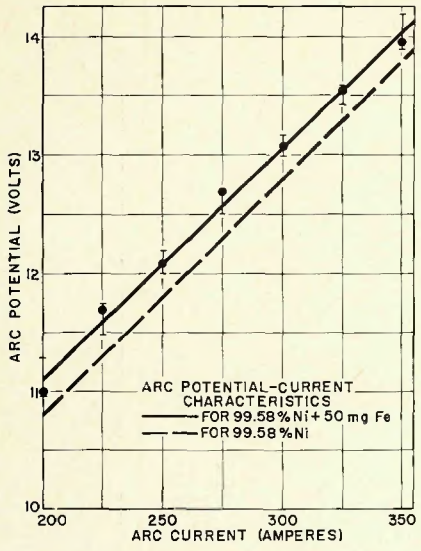

Fig. 11—Arc potential-arc current characteristic for 99.58% Ni + 50 mg

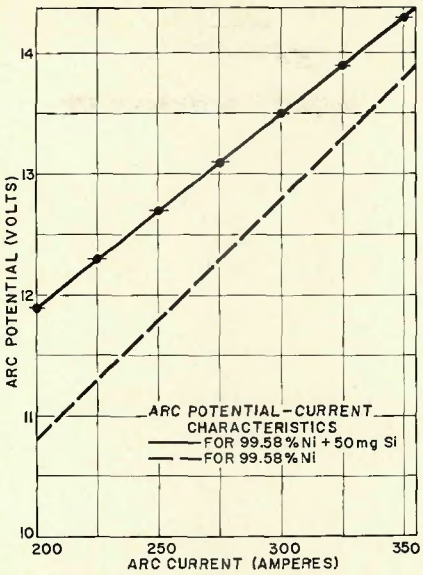

Fig. 12—Arc potential-arc current characteristic for 99.58% Ni + 50 mg

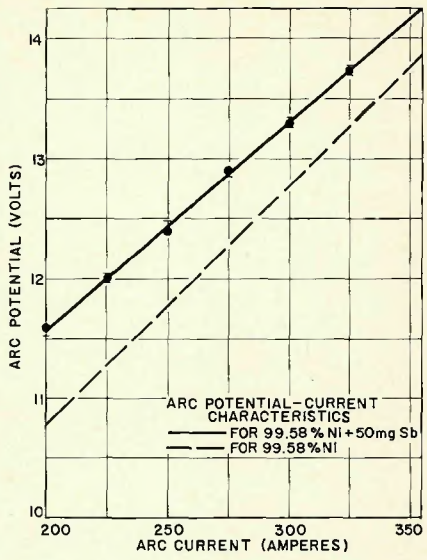

Fig. 13—Arc potential-arc current characteristic for 99.58% Ni + 50 mg

ment remained in solution or became associated with reaction products upon the surface. Since the arc exerts a force on the molten anode, a change in the effective arc gap can occur if a change in the surface tension of the liquid alters the contour of the surface of the weld pool. This arc force has been investigated.[25, 26, 27] However, neither the influence of the anode composition upon the magnitude of arc force, nor upon the surface contour of the weld pool has been investigated quantitatively.

High speed movies taken during this phase of the study revealed some differences in the plasma configuration among the eleven trials. However, these differences were not significant enough to make a quantitative analysis possible. But some of the movies did show differences in puddle contour believed to result from differences in surface tension. In addition, various unidentifiable reaction products were observed on the surface of the molten pool.

Thus although analysis of both the data obtained from the characteristic curves as presented in Table 6 and the high speed motion pictures of the plasma revealed that the arc is indeed sensitive to the anode composition, the mechanism or mechanisms by which the individual elements influence the arc is not clear. All efforts to relate the data obtained from the characteristic curves to the physical properties of the alloying additions mentioned above failed. Therefore, it must be concluded that the observed influence of minor alloying additions on the characteristics of a welding arc may involve complex interactions not anticipated in the design of this experiment. It is entirely possible that the mechanisms are too complex to be resolved until more accurate values for properties listed and for others not considered become available.

Conclusions

1. The arc in a GTA process is sensitive to the anode composition.

2. The arc potential at a given current and arc length is altered by slight changes in the composition of the anode.

3. The slope of the arc potential-arc current characteristic curve is changed by minor additions of alloying element to the anode.

4. No satisfactory model could be formulated to explain observed influence of various elements studied on characteristics of GTA process.

References

1. Jackson, C., "Science of Arc Welding," 1959 Adams Lecture, WELDING JOURNAL, 39 (4-6), Research Suppl., 129-s to 140-s, 177-s to 190-s, 225-s to 230-s (1960).

2. Krammer, P. A., Masubuchi, K., and Monroe, R. E., "Cracking in High Strength Steel Weldments—a Critical Review," DMIC Report 197, Defense Metals Information Center, Battelle Memorial Institute, Columbus, Ohio. February 1964.

3. Pease, G. H., "The Practical Welding Metallurgy of Nickel and High Nickel Alloys," WELDING JOURNAL, 36 (7), 330-s to 334-s (1957).

4. Goodwin, G. M., "The Effect of Minor Elements on the Hot Cracking of Iconel 600," Ph.D. Thesis, Department of Materials Engineering, Rensselaer Polytechnic Institute, Troy, New York, June 1968.

5. Proceedings of a Symposium Sponsored by the Welding Research Council, "Effects of Minor Elements on the Weldability of High-Nickel Alloys," Welding Research Council, July 1969.

6. Oyler, G. W., Matuszesk, R. A., and Garr, C. R., "Why Some Heats of Stainless Steel May Not Weld," WELDING JOURNAL, 46 (12), 1006 to 1011 (1967).

7. Ludwig, H. C., "Current Density and Anode Spot Size in the Gas Tungsten Arc," WELDING JOURNAL, 47 (5), 234-s to 240-s (1968).

8. Spraragen, W., and Lengyel, B. A., "Physics of the Arc and the Transfer of Metal in Arc Welding, A Review of the Literature to February 1942," WELDING JOURNAL, 22 (1), 2-s to 42-s (1943).

9. Lancaster, J. F., "Energy Distribution in Argon-Shielded Welding Arcs," *British Welding Journal*, 1 (9), 412-426 (1954).

10. Goldman, K., "Electric Arcs in Argon," *Physics of the Welding Arc—A Symposium*, 17-22, The Institute of Welding, London (1966).

11. Nestor, O. H., "Heat Intensity and Current Density Distributions at the Anode of High Current, Inert Gas Arcs," *J. Appl. Phys.*, 33 (5), 1638-1648 (1962).

12. Olsen, H. N., "Thermal and Electrical Properties of an Argon Plasma," *The Physics of Fluids*, 2 (6), 614-623 (1959).

13. Cobine, J. D., and Burger, E. E., "Analysis of Electrode Phenomena in the High-Current Arc," *J. Appl. Phys.*, 26 (7), 895-900 (1955).

14. Finkelnburg, W., *The High Current Carbon Arc*, FIAT Final Report 1052, Office of Military Government for Germany (U.S.), Field Information Agency, Technical, (1946).

15. Goldman, K., and White, E. S., "Effect of Anode Material on Arc Mechanism," *British Welding Journal* 430-434, Sept. (1965).

16. Skolnik, M., & Jones, T. B., "Characteristics of High Current Tungsten Arc in Argon, Helium, and Their Mixtures," *J. Appl. Phys.*, 23 (6), 643-652 (1952).

17. Morris, A. D., Gore, W. C., "Analysis of the Direct-Current Arc," WELDING JOURNAL, 35 (3), 137-s to 144-s (1956).

18. Rabkin, D. M., "Research Into the Energetics of Regions Close to the Electrodes of Powerful Welding Arcs," *Avt. Svarka*, No. 2, (1951).

19. Savage, W. F., Lundin, C. D., and Goodwin, G. M., "An Effect of Shielding Gas on Penetration in Iconel Weldments," WELDING JOURNAL, 47 (7), 313-s (1968).

20. Dickinson, D. W., Private Communication, Rensselaer Polytechnic Institute, December 1969.

21. Handbook of Chemistry and Physics, 46th Edition, the Chemical Rubber Publishing Company, Cleveland, Ohio (1965).

22. Fomenko, V. S., *Handbook of Thermionic Properties*, authorized translation, Plenum Press Data Division, New York, N. Y. (1966).

23. Mantel, W., "Considerations on the Importance of the Physical Processes in the Welding Arc," *Schweissen and Schneiden*, 8 (8), 278-280 (1956).

24. Wilkinson, J. B. and Milner, D. R., "Heat Transfer From Arcs," *British Welding Journal*, 115-128, Feb. (1960).

25. Easton, E. C., Lucas, F. B., and Creedy, F., "High Velocity Streams in the Vacuum Arc," *Electrical Engineering*, 1454-1460, Nov. (1934).

26. Reed, T. B., "Determination of Streaming Velocity and Flow of Heat and Mass in High-Current Arcs," *J. Appl. Phys.*, 31 (11), 2048-2052, (1960).

27. Wells, A. A., "A Momentum Principle for Arc Force," *British Welding Journal*, April, 227-231 (1962).